Repetitive transcranial magnetic stimulation increases neurological function and endogenous neural stem cell migration via the SDF-1α/CXCR4 axis after cerebral infarction in rats

YUGUO DENG, FENG GUO, XIAOHUA HAN and XIAOLIN HUANG

Department of Rehabilitation, Tongji Hospital, Tongji Medical College, Huazhong University of Science and Technology, Wuhan, Hubei 430030, P.R. China

Received December 9, 2020; Accepted June 9, 2021

DOI: 10.3892/etm.2021.10469

Abstract. Neural stem cell (NSC) migration is closely associated with brain development and is reportedly involved during recovery from ischaemic stroke. Chemokine signalling mediated by stromal cell-derived factor 1α (SDF-1α) and its receptor CXC chemokine receptor 4 (CXCR4) has been previously documented to guide the migration of NSCs. Although repetitive transcranial magnetic stimulation (rTMS) can increase neurological function in a rat stroke model, its effects on the migration of NSCs and associated underlying mechanism remain unclear. Therefore, the present study investigated the effects of rTMS on ischaemic stroke following middle cerebral artery occlusion (MCAO). All rats underwent rTMS treatment 24 h after MCAO. Neurological function, using modified Neurological Severity Scores and grip strength test and NSC migration, which were measured using immunofluorescence staining, were analysed at 7 and 14 days after MCAO, before the protein expression levels of the SDF-1α/CXCR4 axis was evaluated using western blot analysis. AMD3100, a CXCR4 inhibitor, was used to assess the effects of SDF-1α/CXCR4 signalling. In addition, neuronal survival was investigated using Nissl staining at 14 days after MCAO. It was revealed that rTMS increased the neurological recovery of rats with MCAO, facilitated the migration of NSC, augmented the expression levels of the SDF-1α/CXCR4 axis and decreased neuronal loss. Furthermore, the rTMS-induced positive responses were significantly abolished by AMD3100. Overall, these results indicated that rTMS conferred therapeutic neuroprotective properties, which can restore neurological function after ischaemic stroke, in a manner that may be associated with the activation of the SDF-1α/CXCR4 axis.

Correspondence to: Professor Xiaolin Huang, Department of Rehabilitation, Tongji Hospital, Tongji Medical College, Huazhong University of Science and Technology, 1095 Jiefang Avenue, Wuhan, Hubei 430030, P.R. China
E-mail: xiaolinh2006@126.com

Key words: repetitive transcranial magnetic stimulation, transient focal cerebral ischaemia, neural stem cells migration, stromal cell-derived factor 1α/CXC chemokine receptor 4

Introduction

Neural stem cells (NSCs) are self-renewing, multipotent cells that are located in two vital neurogenic niches: The subventricular zone (SVZ) and the subgranular zone of the adult brain (1). Following ischaemic insult, NSCs in the SVZ proliferate, divert from their physiological migration path and move directly to the lesioned brain area, where they differentiate, mature and functionally integrate into the neural circuits (2). However, this neuroregeneration process is typically inadequate and transient, leading to ineffective neurological function recovery (3). A number of studies have shown that promoting endogenous stem cell migration could improve the neurological recovery of rats with MCAO (4,5). Furthermore, increased endogenous stem cell migration could be evidenced by the presence of recently divided (5-bromo-20-deoxyuridine (BrdU)-labeled) and immature neuronal (doublecortin (DCX)-positive) cells in the injured area in cerebral ischaemic rats (4,5). In addition, another study has reported that specific ablation of DCX-expressing cells suppressed neuromigration in adult mice and decreased neurological recovery in mouse stroke models (6). Therefore, these previous results suggest that the migration of NSCs is critical to stroke recovery.

Repetitive transcranial magnetic stimulation (rTMS) is a non-invasive technique that delivers magnetic pulses through the skull to induce electrical or electromagnetic currents in selective cortical tissues, leading to changes in cortical excitability (7). It has been widely applied for the functional treatment of patients with stroke (8,9), though the mechanisms underlying its beneficial effects remain poorly elucidated. DCX is a microtubule-associated protein that is expressed almost exclusively in cytoplasm of the newly formed neural cells and in migrating neuroblasts in the adult brain (10,11). Using an intracerebral haemorrhage mouse model, a previous study (12) demonstrated that rTMS significantly increased the number of DCX-positive cells in the injured basal ganglia, suggesting its influence on the migration of endogenous stem cells. Additionally, electromagnetic field stimulation has been shown to increase the migration of NSCs from the SVZ

into demyelinated lesions in rats with multiple sclerosis (13). However, further studies are required to explore whether rTMS can promote the migration of NSCs *in vivo* in the SVZ and to explore the mechanism underlying the response following cerebral infarction in rats.

Stromal cell-derived factor 1α (SDF-1α) and its affinity receptor CXC chemokine receptor 4 (CXCR4) are highly expressed in the central nervous system during the developmental process (14). Previous studies revealed that mice deficient in either the expression of SDF-1α or CXCR4 receptors exhibited ectopic navigation of neuronal precursor cells, resulting in the abnormal development of the cortex in the embryonic brain (15-18). During the generation of the hippocampal dentate gyrus (DG), a primary dentate neuroepithelium gives rise to a proliferative cell population that streams along the ventral surface of developing hippocampus to take up a position in the hilus of the DG (14,16). Without functional CXCR4, the number of proliferating cells in the migratory stream is reduced. Therefore, cells fail to reach the forming DG in sufficient numbers, resulting in the failure of DG morphogenesis (17). Normally, during the development of cerebellum, granule cell progenitors are generated in the rhombic lip and then migrate rostromedially along the surface of the cerebellar anlage, forming the external granule cell layer (18). In SDF-1α- or CXCR4-deficient brains of mouse embryos, cells appear to migrate incorrectly from the proliferative external granule cell layer, resulting in the ectopic positioning of granule cells in the Purkinje cell layer, leading to a disorganized cerebellar (19). Following cerebral ischaemia, SDF-1α, which is secreted by astrocytes and endothelial cells surrounding the infarct area, attracts stem cells. CXCR4 is mainly expressed on neural progenitor cells and stroke-induced neuroblasts (20). CXCR4-positive cells migrate along the chemokine gradient of SDF-1α, scaffolded by vessels, corpus callosum and glial cells and are involved in the regulation of axonal outgrowth and patterning, synaptic function and remodelling (21). Some rehabilitation measures have been demonstrated to increase neurological function and augment the migration of endogenous NSCs via the SDF-1α/CXCR4 axis in rats stroke models (4,5). The protein expression levels of CXCR4 are significantly increased in bone marrow mesenchymal stem cells, which enhance cell migration *in vitro* after external electric current stimulation (22,23). In addition, electrical stimulation increases SDF-1α concentrations and enhances the migration of transplanted bone marrow stromal cells to the infarcted areas of rats with stroke (24). However, the effects of rTMS on the expression levels of SDF-1α and CXCR4 in rats after stroke remain unknown.

Cerebral infraction results in neuronal death and therefore, protective approaches against neuronal loss in the penumbra are sorted after. The SDF-1α/CXCR4 axis has conflicting reported functions in neuronal survival, depending on the conditions. An *in vitro* study previously demonstrated that SDF-1α can promote the survival of cortical neurones (25). By contrast, the CXCR4 antagonist AMD3100 has been shown to attenuate inflammatory responses and reduce brain damage in mice following acute ischaemic stroke (26). In addition, another CXCR4 antagonist, CX549, effectively suppresses the inflammatory response and increases neuronal survival, contributing to post-stroke behavioural recovery (27). Previous studies indicated that rTMS not only promotes cell proliferation and inhibits apoptosis in oxygen- and glucose-deprived neuronal cells (28), but also suppresses neuronal degeneration in the peri-infarct region in rats following stroke (29). However, the role of SDF-1α/CXCR4 signalling in the rTMS-mediated protection of neurones in cerebral ischaemic rats remains unknown.

The present study explored whether rTMS could rescue middle cerebral artery occlusion (MCAO)-induced functional impairment by producing a more favourable microenvironment for NSC migration and neuronal survival. Moreover, the role of the SDF-1α/CXCR4 axis in this process was explored.

Materials and methods

Animals and groups. A total of 135 adult male Sprague-Dawley rats (age, 8 weeks; Jingda Bioengineering Co., Ltd., Hunan, China) weighing 210-230 g, were used. The rats were housed in controlled conditions (environment temperature of 25±2˚C, ambient humidity of 50±10%, 12-h light/dark cycle) and were provided with *ad libitum* access to food and water. Randomization was enforced by assigning a number to each rat, and a random number generator was implemented to divide animals into the experimental groups. Rats were divided into sham (S), MCAO (M), rTMS + MCAO (R), rTMS + MCAO + AMD3100 (RA) and MCAO + AMD3100 (MA) groups. These five groups were subdivided further into subsets at two time points, namely 7 and 14 days after MCAO. The present animal study was approved by The Animal Experimentation Ethics Committee of Tongji Hospital (approval. no. 2017609; Wuhan, China) and all treatments conformed to the National Institutes of Health Guide for the Care and Use of Laboratory Animals (Publication no. 80-23; revised 1996). The rats were sacrificed at 7 days (n=11 for each subgroup) or 14 days (n=16 for each subgroup) after MCAO depending on the experimental schedule. In total, six rats in each subgroup were used for immunofluorescence staining and five were used for western blot analysis for both 7 and 14 days. Additionally, Nissl staining was performed in rats (n=5) in the 14-day subgroups.

Focal ischaemic stroke model of rat. A stroke model was established by intraluminally occluding the right middle cerebral artery in rats according to the procedure used by Longa *et al* (30). After being anaesthetized with 5% isoflurane inhalation for induction and 2.5% for maintenance (RWD Life Science Co., Ltd.), a nylon suture thread was inserted into the right internal carotid artery to block blood supply for 90 min as described in a previous study (31). The sham group was subjected to external carotid artery ligation only. During the surgery and recovery period, the rat body temperature was maintained at 37±0.5˚C by a heat lamp. The neurological deficit score (0, no deficit; 1, failure to stretch the left forepaw fully; 2, circling to the left; 3, falling to the left; and 4, no spontaneous gaits with abnormal consciousness) was assessed 4 h after the operation and rats were selected based on a score of 2-3 (30).

Modified neurological severity score (mNSS). The mNSS (32) evaluation was performed at 1, 7 and 14 days after surgery, where the parameters assessed included movement, sense of

touch, reflexes and balance indications. The measures were rated on a scale of 0 to 18 (32), with normal marked as 0 and the most severe deficits marked as 18. Behavioural tests were performed by blinded observers (FG and XHH).

Grip strength metric. On days 1, 7 and 14 post-ischaemia, the forepaw strength of rats was measured using a grip strength meter (Ugo Basile SRL). The rats were trained to grasp the grid with their forelimbs whilst being tugged backwards from the base of tail. After being trained on three successive daily trials before the surgery, the rats were allowed to grasp the meter grid with their forepaws and then pulled carefully from the tail until they released the apparatus. The test was repeated five times per rat with 1-h intervals in between. The average force exerted by the bilateral forepaws was determined from the recorded values. The mean of all five readings was calculated and used for statistical analyses. The grip strength test process and results analysis were performed as previously described (33).

rTMS treatment. At 1 day after ischaemic stroke, conscious rats received rTMS administration by a magnetic stimulator (YRD-CCI, Wuhan Yiruide Medical Equipment New Technology Co., Ltd.) with a 6-cm diameter figure-eight coil. The stimulation site was placed over the ipsilateral primary motor cortex. Richter *et al* (34) previously observed that 45˚ in relation to the standard lateral orientation is the optimal direction for stimulation. Therefore, this stimulus orientation was used. After the rats were fixed on an instrument in a standing position without resistance, they received rTMS once a day for 7 or 14 consecutive days with the following parameters: 10-Hz frequency; 3-sec duration; 50-sec training interval; 10 successive training episodes; 300 pulses; and 120% rest motor threshold (RMT) intensity. The RMT was recorded from the gastrocnemius muscle of the left hind limb using a TMS (Wuhan Yiruide Medical Equipment New Technology Co., Ltd.) as previously described (35). The RMT was defined as the lowest intensity of the TMS able to elicit a motor-evoked potential with amplitudes ≥15 μv at least 5/10 times (36). The rTMS parameters were set based on a previous study according to their efficacy and feasibility (37).

Bromodeoxyuridine and AMD3100 administration. To identify proliferating cells, 5-bromo-20-deoxyuridine [BrdU; 50 mg/kg; intraperitoneal (i.p.) injection; cat. no. B5002; Sigma-Aldrich; Merck KGaA] was administered. For the 7-day subgroups, rats were injected with BrdU every 4 h continuously three times after the last rTMS treatment (7 days after surgery) and then euthanized within 4 h after the last BrdU injection (38). For the 14-day subgroups, rats were administered with BrdU once daily for 7 consecutive days from 24 h post-surgery (39). The CXCR4 receptor antagonist AMD3100 (cat. no. HY-10046; MedChemExpress) was also used in the MA and RA groups. Rats in the MA and RA groups received an AMD3100 (medium saline; 2 mg/kg; i.p.) injection every other day from 2 days after MCAO until euthanasia according to previous reports (4).

Tissue preparation. The specimens were embedded in Optimum Cutting Temperature (cat. no. G6059-110ML; Wuhan Servicebio Technology Co., Ltd.) compound for immunofluorescence analysis, whilst brain samples were paraffin-embedded for Nissl staining. At 7 or 14 days after MCAO, six rats were deeply anaesthetized with 5% isoflurane inhalation induction and 2.5% maintenance (RWD Life Science Co., Ltd.) for 10 min. During this time the rats became unconscious and were insensitive to tail pinch. They were then perfused transcardially with saline and 4% paraformaldehyde at 4˚C for 30 min. The brain tissues were then removed and kept in the same fixative overnight at 4˚C and then incubated in 20 and 30% sucrose consecutively at 4˚C for 3 days dehydration. Subsequently, the brains were embedded in Optimum Cutting Temperature and then cut into 30-μm thick free-floating coronal sections using a cryostat (CM1900; Leica Microsystems GmbH) for immunofluorescence.

At 14 days after surgery, brain samples (n=5) were collected by transcardial perfusion, fixed in paraformaldehyde, dehydrated in sucrose as aforementioned, paraffin-embedded and cut into 4-μm thick slices in the coronal plane (Leica 2035; Leica Microsystems GmbH) for Nissl staining. To be more representative, as referred by a previous report, every sixth slice (40) containing the cerebral infarction was collected, including the cortex and striatum (0.3-1.2 mm behind the bregma).

Immunofluorescence staining. To prepare the slices for BrdU labelling, the free-floating brain sections were washed in PBS three times and denatured in 2 N HCl for 25 min at 37˚C and neutralized with 0.1 M borate solution for 15 min. The free-floating sections were blocked in buffer (10% normal donkey serum and 0.3% Triton X-100 in PBS; pH 7.5; cat. no. ANT051; Wuhan Antejie Biotechnology Co., Ltd. and cat. no. WGT8200; Wuhan Servicebio Technology Co., Ltd.) for 2 h at room temperature and then incubated with a mixture of primary antibodies in 5% donkey serum and PBS overnight at 4˚C. Primary antibodies included rat anti-BrdU (1:100; cat. no. ab6326; Abcam) and goat anti-DCX (1:100; cat. no. sc-8066; Santa Cruz Biotechnology, Inc.). The following day, the primary antibodies were washed and replaced with the secondary antibodies (1:400 for both; Thermo Fisher Scientific, Inc.), TRITC 593-conjugated donkey anti-rat (to conjugate BrdU; cat. no. A18744) and Alexa Fluor 488-labelled donkey anti-goat (to link DCX; cat. no. A-11055; Thermo Fisher Scientific, Inc.) for 2 h at room temperature before rinsing with PBS. Slides were mounted with a DAPI-containing anti-quenching agent (cat. no. AR1177; Wuhan Boster Biological Technology, Ltd.) and sealed with a coverslip. Images were captured with a confocal laser-scanning microscope (magnification x200; Olympus Corporation). Subsequently, two randomly selected regions in the ipsilateral SVZ were observed per section, where the number of BrdU/DCX co-labelled positive cells were identified in the ipsilateral brain area from the SVZ to the ischaemic cortex under a x20 objective in a blinded manner using the ImageJ version 1.50 (National Institutes of Health) software and the average values per slide were recorded. The mean value of three sections in each rat was processed. The results were expressed as the number of labelled cells.

Western blot analysis. Peri-infarct cortical tissue samples from subset groups (n=5) at 7 and 14 days were collected for

western blot analysis. Total proteins were extracted with a Teflon-glass homogenizer in ice-cold homogenization medium containing 1 mM PMSF (Beyotime Institute of Biotechnology) in chilled RIPA buffer (cat. no. P0013B; Beyotime Institute of Biotechnology). The bicinchoninic acid (BCA) protein assay kit (Beyotime Institute of Biotechnology) was employed to estimate the protein concentrations, as detailed in a previous study (37). A total of 40 μg protein per lane was separated using 10% SDS-PAGE gels and then transferred onto PVDF membranes. Subsequently, membranes were blocked with TBST (0.1% Tween-20 in TBS) containing 5% non-fat milk powder for 1 h at room temperature and then incubated overnight at 4˚C with the following primary antibodies: Rabbit anti-SDF-1α (1:300; cat. no. bs-4938R; Bioworld Technology, Inc.) and rabbit anti-CXCR4 antibody (1:300; cat. no. ab181020; Abcam). Next, membranes were washed in 0.1% TBST three times, incubated with associated horseradish peroxidase linked secondary antibodies (1:5,000; cat. no. BA1054; Wuhan Boster Biological Technology, Ltd.) for 1 h at room temperature and washed in 0.1% TBST three times. Blots were visualized using the ECL western blot detection kit (Thermo Fisher Scientific, Inc.). The bands were examined using Gel-Pro Analyzer version 4.0 software (Media Cybernetics, Inc.). The test was repeated in triplicate.

Nissl staining. Nissl staining was performed according to the standard procedure (41). Briefly, after being dewaxed in the xylene and rehydrated in the descending concentration gradient ethanol, the sections were stained with 0.1% cresyl violet acetate (Sigma-Aldrich; Merck KGaA) for 40 min at 60˚C, before they were rinsed, dehydrated in the ascending concentration gradient ethanol and cleared in the xylene. Next, sections were cover slipped and identified under a light microscope (magnification x400; DM2500; Leica Microsystems GmbH) and the area of the penumbra was outlined according to the staining colour and arrangement difference under the x10 objective of the microscope. Images were captured and cell counting was performed with a x40 objective. A total of five randomly selected fields for each coverslip were examined, three sections in each rat were taken before the average values were calculated. Surviving neurones were calculated using Image-Pro Plus version 6.0 (Media Cybernetics, Inc.) software in a blinded manner with reference to the method of Ji *et al* (42). The Nissl bodies (blue) staining in neural cells were clearly visible and distinct. Cells with Nissl staining in the cytoplasm and prominent nucleoli were identified as surviving neurones, whilst cells with shrunken shape, cavitation around the nucleus or loss of Nissl substance were considered damaged (43). Only whole neurones with visible nuclei were counted. The results are expressed as the number of viable neurones (Nissl-positive cells) in the penumbra.

Statistical analysis. Values are shown as the means ± standard error of the mean. All analyses were performed using SPSS version 19 (IBM Corp.). GraphPad Prism version 6.0 software (GraphPad Software, Inc.) was used to generate graphics. For multiple comparisons, data were subjected to a one-way analysis of variance (ANOVA) followed by Bonferroni post hoc comparison. $P<0.05$ was considered to indicate a statistically significant difference.

Results

rTMS improves behavioural outcomes of rats with ischaemic stroke. To assess the neurological function of rats after MCAO, mNSS scoring was used. The mNSS value of the sham-operated rats was 0, where significant differences were not observed in the average scores among the ischaemic rats 1 day after surgery. As shown in Fig. 1A, compared with those in the M and MA groups, rats in the R and RA groups demonstrated significant improvement in the mNSS evaluation at 7 and 14 days after MCAO ($P<0.05$). Rats in the R group exhibited no significant decline in the mNSS scores compared with those in the RA group at 7 days after MCAO. However, a significant increase was observed in the RA group compared with that in the R group at 14 days ($P<0.05$). These results suggest that rTMS alleviated the motor deficiencies in MCAO rats, but AMD3100 abrogated the rTMS-induced response at 14 days.

The purpose of the grip strength test was to evaluate muscle strength and neuromuscular integration corresponding to the forepaw grasping reflex (44). As shown in Fig. 1B, compared with that in sham-operated rats, the grip strength of the rats in the M group significantly decreased ($P<0.01$). Significant differences were not observed in the grip strength test values among the rats 1 day after MCAO. At 7 and 14 days after surgery, the strength of the rats in the R, M and RA groups was increased significantly compared with that in the M, MA and MA groups, respectively ($P<0.01$). Significant differences were not observed between that in the R group and the RA groups at 7 days after MCAO, whilst a significant increase in forepaw power occurred in the R group compared with that in the RA group at 14 days post-ischaemia ($P<0.01$). These results revealed that rTMS increased the muscle strength and neuromuscular integration of MCAO rats. Furthermore, AMD3100 reversed the beneficial effects of rTMS on the forepaw strength of rats at 14 days. In addition, compared with the rats in MCAO group, AMD3100 inhibited the forelimb power recovery of MCAO rats at 7 days.

rTMS enhances the migration of NSCs in rats with ischaemic stroke. To observe migrating SVZ-derived NSCs in the peri-infarction zone (Fig. 2A and B), a BrdU/DCX dual-labelling immunofluorescence test was conducted at different time points of 7 and 14 days. BrdU is a specific maker for cell proliferation, whilst DCX is expressed in newborns and migrating neuroblasts in the adult brain (4,5). Therefore, NSC migration can be quantified by counting the number of BrdU/DCX-immunostained cells (45). The number of BrdU-positive cells in the SVZ increased at 7 and 14 days after MCAO compared with that in the Sham rats (data not shown). Some of the BrdU-positive cells co-expressed DCX, which represented the NSCs diverting from the SVZ. A small number of DCX^+ cells were found in the left lateral SVZ of rats in the M group or in the bilateral SVZ of Sham rats. Thereafter, DCX^+ cells were numerically increased and distributed in the callosum and striatum of the ipsilateral hemisphere at 7 and 14 days after surgery. At 14 days, the $BrdU^+/DCX^+$ cells with elongated dendrites, formed clusters at the SVZ, arranged in a chain-like manner along the ventricle lateral wall, and migrated towards the infarction site (Fig. 2C-2J). As shown in Fig. 3F at 7 days post-ischaemia (Figs. 3F and S1), significantly more

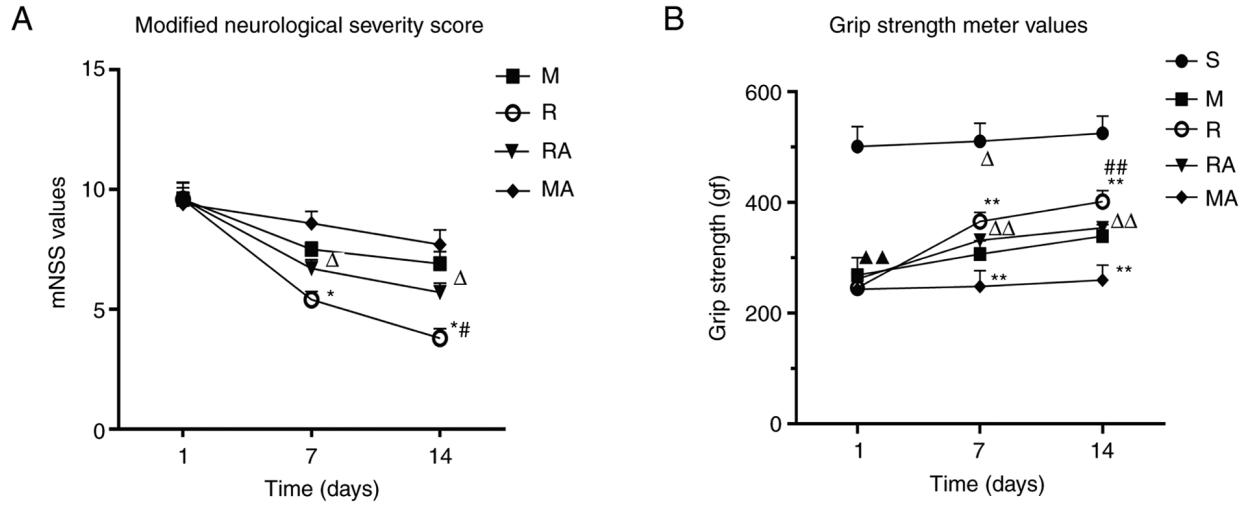

Figure 1. rTMS treatment increases the behavioural performance of rats at 7 and 14 days after MCAO. (A) Recovery of neurological function evaluated by mNSS. (B) Forelimb strength as measured using the grip strength meter. n=10 rats per group. ▲▲P<0.01 vs. S; *P<0.05 and **P<0.01 vs. M; #P<0.05 and ##P<0.01 vs. RA; ΔP<0.05 and ΔΔP<0.01 vs. MA group. mNSS, modified neurological severity scores; MCAO, middle cerebral artery occlusion model; rTMS, repetitive transcranial magnetic stimulation; S, sham; M, MCAO; R, rTMS + MCAO; RA, rTMS + MCAO + AMD3100; MA, MCAO + AMD3100.

$BrdU^+/DCX^+$ cells were observed in the ipsilateral SVZ of the M group compared with those in the S group (P<0.05). In addition, rTMS treatment significantly augmented the number of $BrdU^+/DCX^+$ cells in the R group compared with that in rats in the M group (P<0.05). The number of dual-positive cells in the RA group was significantly increased compared with those in the MA group (P<0.05).

At 14 days post-ischaemia, the numbers of $BrdU^+/DCX^+$ cells increased significantly in the M group compared with those in the S group (P<0.05), the same trend was also observed in the R group compared with that in the M group (P<0.01), in addition to in the R group compared with that in the RA group (P<0.05). However, significant differences were not observed between the numbers in the RA and MA groups (Fig. 3F). These results suggest that 10 Hz rTMS enhanced the ischaemia-induced increases in the number of $BrdU^+/DCX^+$ co-labelled-cells. Additionally, AMD3100 inhibited the beneficial effects of rTMS against MCAO in rats at 14 days but not at 7 days.

rTMS increases the expression levels of proteins in the SDF-1α/CXCR4 axis in the peri-infarction zone after MCAO. To examine the effects of rTMS on the SDF-1α/CXCR4 signaling axis in MCAO rats, western blot analysis was used to observe the protein expression levels of SDF-1α and CXCR4 at 7 and 14 days after MCAO (Fig. 4). The expression levels of SDF-1α and CXCR4 in rats in the M group were significantly upregulated compared with those in the sham group (P<0.05; Fig. 4). Furthermore, the R group displayed significantly increased SDF-1α and CXCR4 expression levels at both 7 and 14 days compared with those in the M group (all P<0.05; Fig. 4A). The expression levels of SDF-1α in the RA group was significantly increased compared with those in the MA group at 7 and 14 days (P<0.05; Fig. 4A). In addition, the expression levels of SDF-1α in the MA group was significantly decreased compared with that in the M group at 14 days (P<0.05; Fig. 4A).

The expression level of CXCR4 was significantly increased in the R group compared with that in the RA group, whilst the same trend was also observed for the M group compared with that in the MA group, in addition to for that in the RA group compared with that in the MA group at both time-points (all P<0.05; Fig. 4B). These results suggest that the SDF-1α/CXCR4 axis was inhibited by AMD3100 and that rTMS could upregulate the expression levels of SDF-1α and CXCR4 in rats following MCAO.

rTMS increases the number of surviving neurones in the ischaemic penumbra. Nissl staining was performed to assess neuronal injury. Since a tendency to behavioural improvement was observed in rats in the R group after 14 days compared with those in the same group after 7 days (data not shown), rats in the R group were selected for Nissl staining after 14 days (Figs. 2A and 5). As shown in Fig. 2A, the injured area (concluded ischemic core and penumbra) mainly was focused on the cerebral cortex and the striatum. Damaged neurones would exhibit the absence of Nissl's bodies, smaller intercellular space and abnormal staining. Neurones were found to be arranged randomly with irregular shapes in the M group (Fig. 5B). The number of $Nissl^+$ neurones per high power field in rats in the M group was significantly decreased compared with that in sham rats (P<0.05; Fig. 5F). By contrast, rTMS significantly alleviated MCAO-induced neuronal loss, as shown by the significantly increased numbers of $Nissl^+$ neurones in the R group compared with those in the M group (P<0.05; Fig. 5F). Statistical analysis also demonstrated that the number of surviving neurones in the MA group was significantly decreased compared with that in the RA group (P<0.05; Fig. 5F). Additionally, significant differences were observed between the R group and RA group and between the M group and MA group (both P<0.05; Fig. 5F). The number of $Nissl^+$ neurons in the R and M group was significantly higher than that in the RA and MA groups, respectively. These results suggest that rTMS can rescue MCAO-induced neuronal damage in the penumbra, whereas this positive response was inhibited by AMD3100.

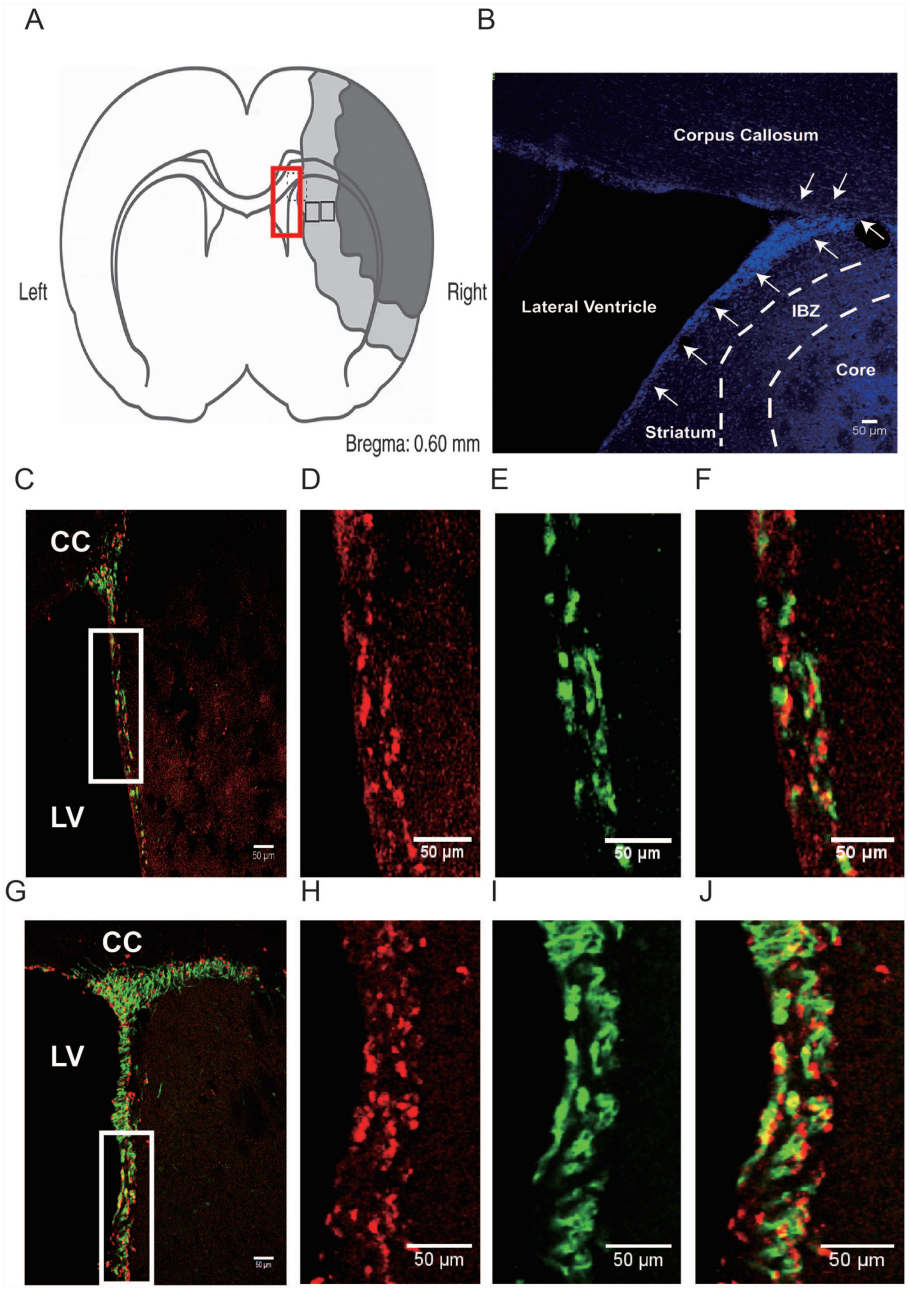

Figure 2. Schematic view of the region of interest and representative confocal images of immunofluorescence staining at 14 days post-surgery. (A) Coronal section representation of an ischaemic rat brain (bregma 0.60 mm). Dark section denotes the ischaemic core, the grey section indicates the ischaemic penumbra and white sections indicate non-ischaemic area. For image analysis, representative fields (rectangle in red colour) in the SVZ and representative fields (rectangle in black colour) in the penumbra were selected. (B) Representative images of immunofluorescence labelling with DAPI (blue) staining in the M group at 7 days post-surgery. The SVZ (white arrows) located between the LV and the striatum. IBZ (penumbra) was defined as an area surrounded by white dashed lines and ischemic core located right side from the right broken line. Magnification x100. (C-J) Representative ipsilateral SVZ zones were subjected to immunofluorescence labelling with BrdU (red) and DCX (green) staining. (C) Representative ipsilateral SVZ zone image from the M group 14 days after surgery. The three columns on the right (D-F) show higher magnification images of the white boxed areas in (C). Images of (D) BrdU+, (E) DCX+, (F) BrdU/DCX dual-positive cells in the M group at 14 days post-surgery. (G) Representative ipsilateral SVZ zone image from the R group 14 days after surgery. The three columns (H-J) show higher magnification images of the white boxed areas in (G). Images of (H) BrdU+, (I) DCX+, (J) BrdU/DCX dual-positive cells in the R group at 14 days post-surgery. Scale bars, 50 μm. CC, corpus callosum; LV, lateral ventricle; SVZ, subventricular zone; IBZ, ischemic boundary zone; Core, infarct core; MCAO, middle cerebral artery occlusion model; rTMS, repetitive transcranial magnetic stimulation; S, sham; M, MCAO; R, rTMS + MCAO; RA, rTMS + MCAO + AMD3100; MA, MCAO + AMD3100; BrdU, bromodeoxyuridine; DCX, doublecortin.

Discussion

The present study demonstrated that high-frequency rTMS facilitated functional recovery from ischaemic stroke in a rat MCAO model, which was associated with enhanced migration of NSCs and reduced neuronal loss in the peri-infarct area. Together with these effects, the protein expression levels of SDF-1α and CXCR4 were significantly increased by 10 Hz rTMS treatment. However, the rTMS-induced changes were significantly inhibited by AMD3100. To the best of our knowledge, the present study demonstrated for the first time that the restorative and neuroprotective effects of rTMS in rats

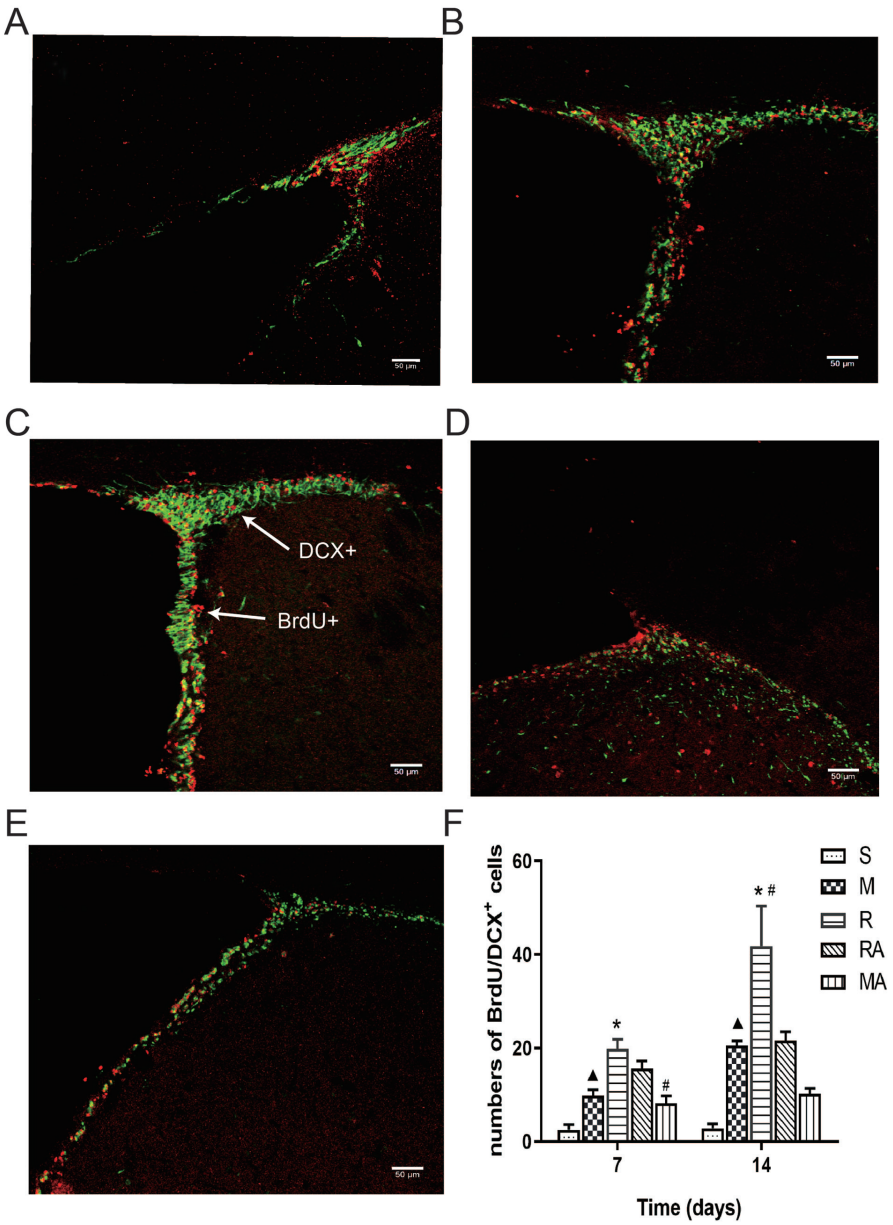

Figure 3. rTMS treatment promotes the migration of neural stem cells in the ipsilateral SVZ at 7 and 14 days after MCAO. Representative confocal images of immunofluorescence staining. Staining in the (A) S group, (B) M group, (C) R group, (D) RA group and (E) MA group at 14 days after ischaemia onset. White arrows indicate examples of colocalized cells. Red represents BrdU and green represents DCX. Magnification, x200; scale bar, 50 μm. (F) Quantification the number of BrdU/DCX dual-positive cells per section in each group. n=6 rats per group. ▲P<0.05 vs. S; *P<0.05 vs. M; #P<0.05 vs. RA. MCAO, middle cerebral artery occlusion model; rTMS, repetitive transcranial magnetic stimulation; S, sham; M, MCAO; R, rTMS + MCAO; RA, rTMS + MCAO + AMD3100; MA, MCAO + AMD3100; BrdU, bromodeoxyuridine; DCX, doublecortin.

following ischaemic stroke may be dependent on the activation of SDF-1α/CXCR4 signalling.

Activating endogenous NSCs to remodel the neural tissue is considered to be an effective therapeutic strategy after cerebral ischemic injury in rats (46). The infarct area was found to be enlarged, where the neurological deficits were more severe, in mice that were depleted of DCX- and BrdU-immunoreactive cells in the SVZ post-ischaemia, suggesting that boosting NSC migration is a potential target for stroke treatment (47). The present study used mNSS values and grip strength to evaluate neurological function, muscular strength and neuromuscular integration in rats following cerebral ischaemia. The results indicated that 10 Hz rTMS significantly restored motor dysfunction and further promoted the migration of NSCs, as evidenced by the significantly increased number of $BrdU^+/DCX^+$ cells in the ipsilateral SVZ compared with that in the M group at 7 and 14 days post-ischaemia. Similar results were found in a previous clinical (9) and preclinical (48) study, indicating that rTMS can increase overall motor function following ischaemic stroke. Exogenous electrical stimulation can confer positive effects on NSC migration *in vitro* (49). Additionally, a previous study also demonstrated that electromagnetic field stimulation can promote the migration of proliferative cells from the SVZ into demyelinated lesions in the corpus callosum in a rat model of multiple sclerosis (13). Therefore, the improvement of motor function observed with rTMS may be associated with the enhancement of NSC migration in rats with ischaemic stroke.

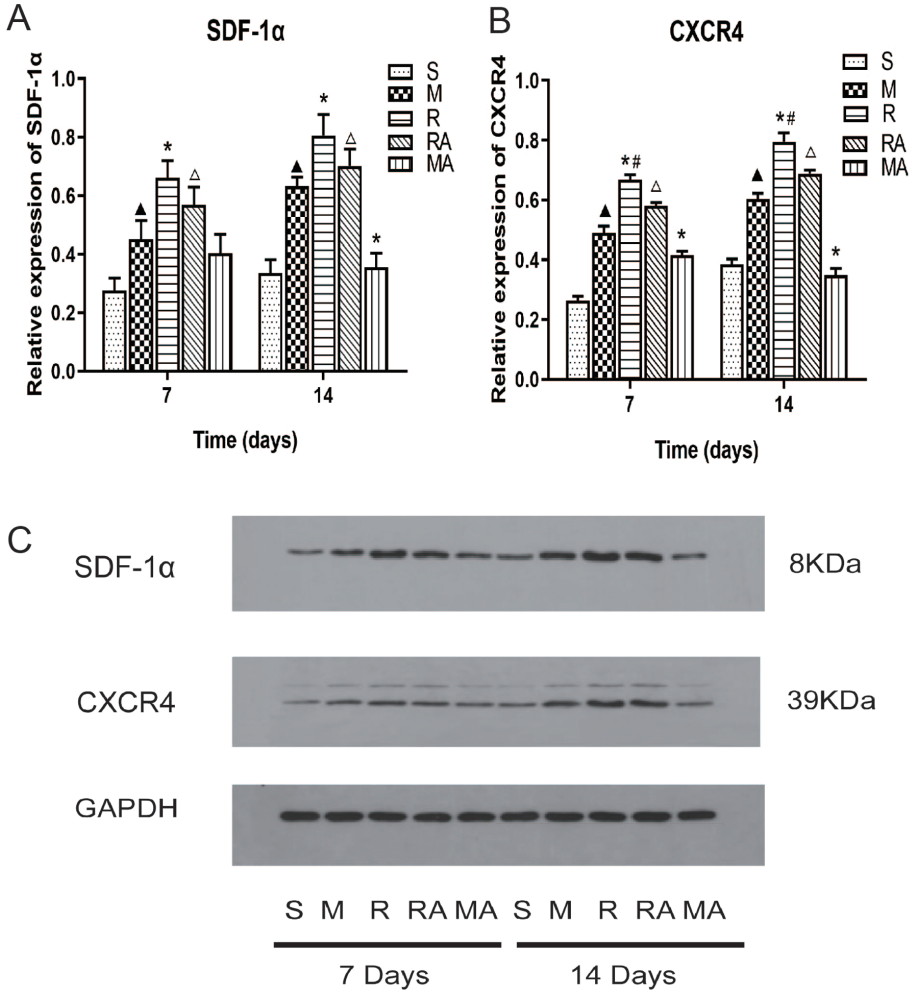

Figure 4. Effects of rTMS on SDF-1α and CXCR4 expression in the ipsilateral tissue at 7 and 14 days after surgery. Protein expression levels of (A) SDF-1α and (B) CXCR4 in the ischaemia samples as determined by western blot analysis. (C) Representative western blotting images of SDF-1α, CXCR4 and GAPDH on gel. n=5 rats per group. ▲P<0.05 vs. S group; *P<0.05 vs. M group; #P<0.05 vs. RA group; △P<0.05 vs. MA group. MCAO, middle cerebral artery occlusion model; rTMS, repetitive transcranial magnetic stimulation; S, sham; M, MCAO; R, rTMS + MCAO; RA, rTMS + MCAO + AMD3100; MA, MCAO + AMD3100; SDF-1α, Stromal cell-derived factor 1α; CXCR4, CXC Chemokine receptor 4.

Chemokines are important factors that regulate cell migration (50). Using a rat model of acute ischemic stroke, a previous study has revealed that SDF-1α and CXCR4 expression levels were upregulated following stroke (51). Overexpression of SDF-1α in the boundary of the infarcted area in rats with ischemic stroke resulted in increased NSCs recruitment in the SVZ (52). Furthermore, SDF-1α/CXCR4 stimulates outward radial migration of neural precursors from adherent neurospheres *in vitro* in a dose-dependent manner after treatment with CXCL12 (SDF-1α) in the medium (53). When CXCR4 receptor-blocking antibodies were applied, the migration of NSCs was also significantly reduced (5). Therefore, SDF-1α/CXCR4 signalling can potentially manipulate the trafficking of endogenous NSCs. Results of the present study demonstrated that rTMS enhanced the expression of SDF-1α and CXCR4, which was accompanied by an increased number of $BrdU^+/DCX^+$ cells at the ischaemic border, in a manner that was susceptible to blockade by AMD3100. Similarly, a previous study observed that electrical stimulation increased SDF-1α concentrations and enhanced the migration of exogenous bone marrow stromal cells to the infarction zone in a rat stroke model (24). In the present study, the AMD3100-induced reduction in SDF-1α and CXCR4 expression resulted in decreased neurological recovery in the RA group at 7 and 14 days after stroke. These results imply that the SDF-1α/CXCR4 axis can contribute to rTMS-mediated recovery of motor dysfunction after stroke in rats. These effects may be explained by the significant reduction in rTMS-induced NSC migration caused by AMD3100 at 14 days post-surgery, thereby significantly attenuating functional recovery. Moreover, the number of $BrdU^+/DCX^+$ cells was significantly increased in the R group compared with that in the RA group, whereas significant differences were not observed between the RA group and MA group at 14 days post ischaemia. These results indicated that AMD3100 inhibited the migration of NSCs following ischaemic stroke and that rTMS may enhance the migration of NSCs via other mechanisms. A previous report indicated that electrical excitation can direct the migration of NSCs via galvanotaxis independent of SDF-1α chemical gradients (54). Nevertheless, data from the present study demonstrated that rTMS enhanced NSC migration in rats following MCAO, possibly by activating the SDF-1α/CXCR4 axis.

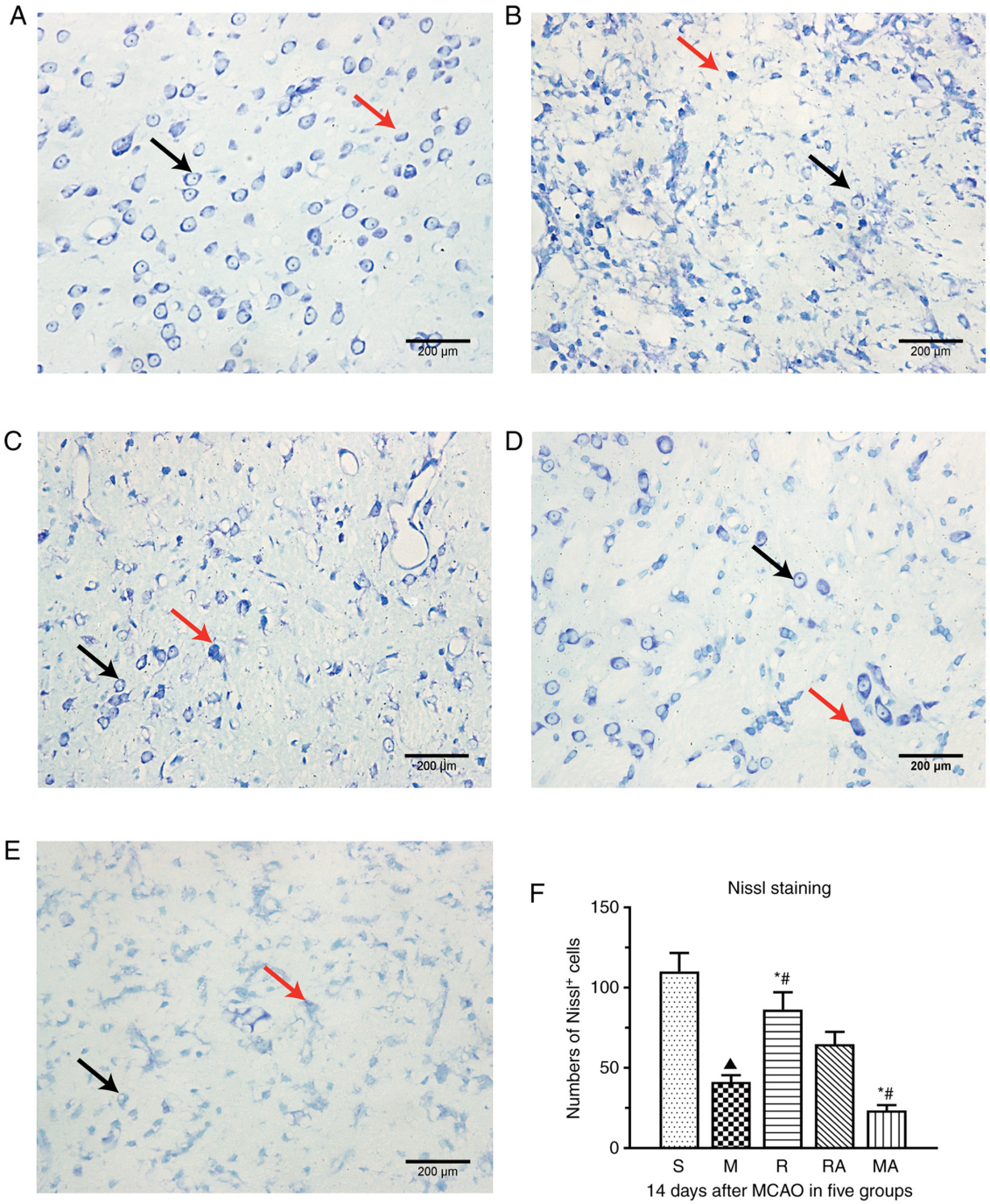

Figure 5. rTMS treatment protects neurones against ischaemic injury in the penumbra at 14 days after surgery. Representative images of Nissl staining in the (A) S, (B) M, (C) R, (D) RA and (E) MA groups (magnification, x400; scale bar, 200 μm). (F) Quantified analysis of Nissl-positive neurones per section in the five groups. Black arrows represent examples of surviving neurones (Nissl-positive cells). Red arrows indicate examples of damaged neurones. n=5 rats per group. ▲P<0.05 vs. S; *P<0.05 vs. M; #P<0.05 vs. RA. MCAO, middle cerebral artery occlusion model; rTMS, repetitive transcranial magnetic stimulation; S, sham; M, MCAO; R, rTMS + MCAO; RA, rTMS + MCAO + AMD3100; MA, MCAO + AMD3100.

The role of SDF-1α in cerebral insults remains under exploration. SDF-1α-overexpression has been found to protect neurones in the penumbra following ischaemic brain insult, resulting in a significantly decreased number of apoptotic cells (52). A study by Chiazza *et al* (55) indicated that activation of the SDF-1α/CXCR4 axis resulted in reduced tissue damage, promoted neuronal survival and improved upper-limb function recovery after post-stroke treatment in MCAO mice. In addition, using Nissl staining, Sun *et al* (56) demonstrated that SDF-1α injection prevents neurones from degenerating in rats following traumatic brain injuries. Another previous study reported that rTMS can enhance neuron survival in the perilesional zone in rats after traumatic brain injury (57). In the present study, rTMS treatment rescued ischaemia-induced neuronal damage in the penumbra. Furthermore, AMD3100 treatment abolished the enhanced survival of neurones in the perilesional area in the R group. A study has previously revealed that the content of SDF-1α is significantly higher in the infarcted striatum of rats after ischaemic stroke (24) and in the anal sphincter of rats (58) after electrical stimulation. Although it is possible

that rTMS use can protects neural cells in the injured area in other ways, such activity may be at least in part attributed to the SDF-1α/CXCR4 axis. The brain is comprised of an intricate neuronal network where various types of cells interact with each other (59). The endogenous neurogenic response is also under the influence of the surrounding microenvironment, such as the optimization of SDF-1α expression and neurotrophins in the penumbra (60,61). Therefore, rTMS may create a favourable microenvironment where surviving neurones and NSCs can synergistically promote functional recovery.

The present study has some limitations. An indirect method was used to evaluate the migration of NSCs instead of measuring the migration distance using another method. For example, SVZ neuroblast migration as evaluated by the distance from the SVZ to the cell cluster nearest to the ischemic area was considered to reflect the migratory distance, where the maximal distance that the SVZ cells covered was measured (62). The influence of rTMS on the proliferation of NSCs also cannot be ruled out. Further studies are required to validate if the migration of NSCs mediated by rTMS is associated with the differentiation of new neurones and if they are fully functional in neural circuits. Although motor-evoked potential measurements were used for determining optimal localization (63), poor localization and the whole brain may be inevitably stimulated because the stimulator coil (6-cm in diameter) was relatively large for the rodent brain. In addition, a previous study suggested that rTMS treatment (10 Hz rTMS stimulation of the ipsilateral motor cortex) promotes cognitive functional recovery after ischaemic stroke in rats by inhibiting apoptosis whilst enhancing neurogenesis in the hippocampus distal to the stimulation site (64). By contrast, another study reported that neurogenesis was not significantly increased after 20 Hz rTMS intervention (the stimulation point was set at the left frontal cortex) in a rat model of chronic psychosocial stress (65). This discrepancy may be attributed to the different stimulating frequencies and animal models used. These results suggest that appropriate parameters for electrical stimulation are important in clinical settings and animal models. It is worth assessing the underlying mechanisms and optimized protocols of rTMS in neurogenesis.

In conclusion, the present study provided new insights into the effects of rTMS on neurological deficits after ischaemic stroke, which suggested that the mechanism may be associated with the enhancement of endogenous NSC migration and neuroprotection. In addition, SDF-1α/CXCR4 signalling may serve a notable role in this process.

Acknowledgements

The authors would like to thank Professor Wang Wei (Department of Neurology, Tongji Hospital, Tongji Medical College, Huazhong University of Science and Technology), for his assistance with the usage of confocal laser-scanning microscope.

Funding

The present study was supported by The National Natural Science Foundation of China (grant. nos. 81702231, 81572238 and 81071601).

Availability of data and materials

The datasets used and/or analysed during the current study are available from the corresponding author on reasonable request.

Authors' contributions

YD performed the majority of the experiments. FG constructed the animal models and analysed the majority of the data. XHa analysed the immunofluorescence staining data and revised the manuscript critically for important intellectual content. XHu contributed to the conception, design, data acquisition, analysis, interpretation and critically revised the manuscript for important intellectual content. YD and XHu confirm the authenticity of all the raw data. All authors have read and approved the final manuscript.

Ethics approval and consent to participate

This animal study was approved by The Animal Experimentation Ethics Committee of Tongji Hospital (approval no. 2017609; Wuhan, China).

Patient consent for publication

Not applicable.

Competing interests

The authors declare that they have no competing interests.

References

1. Sanai N, Tramontin AD, Quiñones-Hinojosa A, Barbaro NM, Gupta N, Kunwar S, Lawton MT, McDermott MW, Parsa AT, Verdugo JM, *et al*: Unique astrocyte ribbon in adult human brain contains neural stem cells but lacks chain migration. Nature 427: 740-744, 2004.
2. Kannangara TS, Carter A, Xue Y, Dhaliwal JS, Beique JC and Lagace DC: Excitable adult-generated GABAergic neurones acquire functional innervation in the cortex after stroke. Stem Cell Rep 11: 1327-1336, 2018.
3. Tsintou M, Dalamagkas K and Makris N: Taking central nervous system regenerative therapies to the clinic: Curing rodents versus nonhuman primates versus humans. Neural Regen Res 15: 425-437, 2020.
4. Luo J, Hu X, Zhang L, Li L, Zheng H, Li M and Zhang Q: Physical exercise regulates neural stem cells proliferation and migration via SDF-1α/CXCR4 pathway in rats after ischemic stroke. Neurosci Lett 578: 203-208, 2014.
5. Zhao S, Qu H, Zhao Y, Xiao T, Zhao M, Li Y, Jolkkonen J, Cao Y and Zhao C: CXCR4 antagonist AMD3100 reverses the neurogenesis and behavioral recovery promoted by forced limb-use in stroke rats. Restor Neurol Neurosci 33: 809-821, 2015.
6. Jin K, Wang X, Xie L, Mao XO and Greenberg DA: Transgenic ablation of doublecortin-expressing cells suppresses adult neurogenesis and worsens stroke outcome in mice. Proc Natl Acad Sci USA 107: 7993-7998, 2010.
7. Hummel FC and Cohen LG: Non-invasive brain stimulation: A new strategy to improve neurorehabilitation after stroke? Lancet Neurol 5: 708-712, 2006.
8. Yuan X, Yang Y, Cao N and Jiang C: Promotion of poststroke motor-function recovery with repetitive transcranial magnetic stimulation by regulating the interhemispheric imbalance. Brain Sci 10: 648, 2020.
9. Fisicaro F, Lanza G, Grasso AA, Pennisi G, Bella R, Paulus W and Pennisi M: Repetitive transcranial magnetic stimulation in stroke rehabilitation: Review of the current evidence and pitfalls. Ther Adv Neurol Disord 12: 1278099885, 2019.

10. Gleeson JG, Lin PT, Flanagan LA and Walsh CA: Doublecortin is a microtubule-associated protein and is expressed widely by migrating neurons. Neuron 23: 257-271, 1999.
11. Couillard-Despres S, Winner B, Schaubeck S, Aigner R, Vroemen M, Weidner N, Bogdahn U, Winkler J, Kuhn HG and Aigner L: Doublecortin expression levels in adult brain reflect neurogenesis. Eur J Neurosci 21: 1-14, 2005.
12. Cui M, Ge H, Zeng H, Yan H, Zhang L, Feng H and Chen Y: Repetitive transcranial magnetic stimulation promotes neural stem cell proliferation and differentiation after intracerebral hemorrhage in mice. Cell Transplant 28: 568-584, 2019.
13. Sherafat MA, Heibatollahi M, Mongabadi S, Moradi F, Javan M and Ahmadiani A: Electromagnetic field stimulation potentiates endogenous myelin repair by recruiting subventricular neural stem cells in an experimental model of white matter demyelination. J Mol Neurosci 48: 144-153, 2012.
14. Li M and Ransohoff RM: Multiple roles of chemokine CXCL12 in the central nervous system: A migration from immunology to neurobiology. Prog Neurobiol 84: 116-131, 2008.
15. Ho SY, Ling TY, Lin HY, Liou JT, Liu FC, Chen IC, Lee SW, Hsu Y, Lai DM and Liou HH: SDF-1/CXCR4 signaling maintains stemness signature in mouse neural stem/progenitor cells. Stem Cells Int 2017: 2493752, 2017.
16. Hatami M, Conrad S, Naghsh P, Alvarez-Bolado G and Skutella T: Cell-biological requirements for the generation of dentate gyrus granule neurons. Front Cell Neurosci 12: 402, 2018.
17. Lu M, Grove EA and Miller RJ: Abnormal development of the hippocampal dentate gyrus in mice lacking the CXCR4 chemokine receptor. Proc Natl Acad Sci USA 99: 7090-7095, 2002.
18. Zanin JP, Abercrombie E and Friedman WJ: Proneurotrophin-3 promotes cell cycle withdrawal of developing cerebellar granule cell progenitors via the p75 neurotrophin receptor. Elife 5: e16654, 2016.
19. Ma Q, Jones D, Borghesani PR, Segal RA, Nagasawa T, Kishimoto T, Bronson RT and Springer TA: Impaired B-lymphopoiesis, myelopoiesis, and derailed cerebellar neuron migration in CXCR4- and SDF-1-deficient mice. Proc Natl Acad Sci USA 95: 9448-9453, 1998.
20. Tsai LK, Wang Z, Munasinghe J, Leng Y, Leeds P and Chuang DM: Mesenchymal stem cells primed with valproate and lithium robustly migrate to infarcted regions and facilitate recovery in a stroke model. Stroke 42: 2932-2939, 2011.
21. Sanchez AB, Medders KE, Maung R, Sanchez-Pavon P, Ojeda-Juárez D and Kaul M: CXCL12-induced neurotoxicity critically depends on NMDA receptor-gated and L-type Ca^{2+} channels upstream of p38 MAPK. J Neuroinflammation 13: 252, 2016.
22. Hwang SJ, Song YM, Cho TH, Kim RY, Lee TH, Kim SJ, Seo YK and Kim IS: The implications of the response of human mesenchymal stromal cells in three-dimensional culture to electrical stimulation for tissue regeneration. Tissue Eng Part A 18: 432-445, 2012.
23. Wang X, Gao Y, Shi H, Liu N, Zhang W and Li H: Influence of the intensity and loading time of direct current electric field on the directional migration of rat bone marrow mesenchymal stem cells. Front Med 10: 286-296, 2016.
24. Morimoto J, Yasuhara T, Kameda M, Umakoshi M, Kin I, Kuwahara K, Kin K, Okazaki M, Takeuchi H, Sasaki T, *et al*: Electrical stimulation enhances migratory ability of transplanted bone marrow stromal cells in a rodent ischemic stroke model. Cell Physiol Biochem 46: 57-68, 2018.
25. Nicolai J, Burbassi S, Rubin J and Meucci O: CXCL12 inhibits expression of the NMDA receptor's NR2B subunit through a histone deacetylase-dependent pathway contributing to neuronal survival. Cell Death Dis 1: e33, 2010.
26. Huang J, Li Y, Tang Y, Tang G, Yang GY and Wang Y: CXCR4 antagonist AMD3100 protects blood-brain barrier integrity and reduces inflammatory response after focal ischemia in mice. Stroke 44: 190-197, 2013.
27. Wu KJ, Yu SJ, Shia KS, Wu CH, Song JS, Kuan HH, Yeh KC, Chen CT, Bae E and Wang Y: A novel CXCR4 Antagonist CX549 induces neuroprotection in stroke brain. Cell Transplant 26: 571-583, 2017.
28. Baek A, Kim JH, Pyo S, Jung JH, Park EJ, Kim SH and Cho SR: The differential effects of repetitive magnetic stimulation in an in vitro neuronal model of ischemia/reperfusion injury. Front Neurol 9: 50, 2018.
29. Zong X, Dong Y, Li Y, Yang L, Li Y, Yang B, Tucker L, Zhao N, Brann DW, Yan X, *et al*: Beneficial effects of theta-burst transcranial magnetic stimulation on stroke injury via improving neuronal microenvironment and mitochondrial integrity. Transl Stroke Res 11: 450-467, 2020.
30. Longa EZ, Weinstein PR, Carlson S and Cummins R: Reversible middle cerebral artery occlusion without craniectomy in rats. Stroke 20: 84-91, 1989.
31. Sha R, Zhang B, Han X, Peng J, Zheng C, Zhang F and Huang X: Electroacupuncture alleviates ischemic brain injury by inhibiting the miR-223/NLRP3 pathway. Med Sci Monitor 25: 4723-4733, 2019.
32. Chen J, Sanberg PR, Li Y, Wang L, Lu M, Willing AE, Sanchez-Ramos J and Chopp M: Intravenous administration of human umbilical cord blood reduces behavioral deficits after stroke in rats. Stroke 32: 2682-2688, 2001.
33. Balkaya M, Krober JM, Rex A and Endres M: Assessing post-stroke behavior in mouse models of focal ischemia. J Cereb Blood Flow Metab 33: 330-338, 2013.
34. Richter L, Neumann G, Oung S, Schweikard A and Trillenberg P: Optimal coil orientation for transcranial magnetic stimulation. PLoS One 8: e60358, 2013.
35. Zhang XY, Sui YF, Guo TC, Wang SH, Hu Y and Lu YS: Effect of paired associative stimulation on motor cortex excitability in rats. Curr Med Sci 38: 903-909, 2018.
36. Shin HI, Han TR and Paik NJ: Effect of consecutive application of paired associative stimulation on motor recovery in a rat stroke model: A preliminary study. Int J Neurosci 118: 807-820, 2008.
37. Peng JJ, Sha R, Li MX, Chen LT, Han XH, Guo F, Chen H and Huang XL: Repetitive transcranial magnetic stimulation promotes functional recovery and differentiation of human neural stem cells in rats after ischemic stroke. Exp Neurol 313: 1-9, 2019.
38. Guo F, Han X, Zhang J, Zhao X, Lou J, Chen H and Huang X: Repetitive transcranial magnetic stimulation promotes neural stem cell proliferation via the regulation of MiR-25 in a rat model of focal cerebral ischemia. PLoS One 9: e109267, 2014.
39. Nygren J, Wieloch T, Pesic J, Brundin P and Deierborg T: Enriched environment attenuates cell genesis in subventricular zone after focal ischemia in mice and decreases migration of newborn cells to the striatum. Stroke 37: 2824-2829, 2006.
40. Chen H, Qian K, Chen W, Hu B, Blackbourn LW IV, Du Z, Ma L, Liu H, Knobel KM, Ayala M, *et al*: Human-derived neural progenitors functionally replace astrocytes in adult mice. J Clin Invest 125: 1033-1042, 2015.
41. Zhan L, Yan H, Zhou H, Sun W, Hou Q and Xu E: Hypoxic preconditioning attenuates neuronal cell death by preventing MEK/ERK signaling pathway activation after transient global cerebral ischemia in adult rats. Mol Neurobiol 48: 109-119, 2013.
42. Ji Y, Teng L, Zhang R, Sun J and Guo Y: NRG-1β exerts neuroprotective effects against ischemia reperfusion-induced injury in rats through the JNK signaling pathway. Neuroscience 362: 13-24, 2017.
43. Tan F, Wang J, Liu JX, Wang C, Li M and Gu Y: Electroacupuncture stimulates the proliferation and differentiation of endogenous neural stem cells in a rat model of ischemic stroke. Exp Ther Med 16: 4943-4950, 2018.
44. Meyer OA, Tilson HA, Byrd WC and Riley MT: A method for the routine assessment of fore- and hindlimb grip strength of rats and mice. Neurobehav Toxicol 1: 233-236, 1979.
45. Fu DL, Li JH, Shi YH, Zhang XL, Lin Y and Zheng GQ: Sanhua decoction, a classic herbal prescription, exerts neuroprotection through regulating phosphorylated tau level and promoting adult endogenous neurogenesis after cerebral ischemia/reperfusion injury. Front Physiol 11: 57, 2020.
46. Jin Y, Raviv N, Barnett A, Bambakidis NC, Filichia E and Luo Y: The shh signaling pathway is upregulated in multiple cell types in cortical ischemia and influences the outcome of stroke in an animal model. PLoS One 10: e124657, 2015.
47. Wang X, Mao X, Xie L, Sun F, Greenberg DA and Jin K: Conditional depletion of neurogenesis inhibits long-term recovery after experimental stroke in mice. PLoS One 7: e38932, 2012.
48. Gao F, Wang S, Guo Y, Wang J, Lou M, Wu J, Ding M, Tian M and Zhang H: Protective effects of repetitive transcranial magnetic stimulation in a rat model of transient cerebral ischaemia: A microPET study. Eur J Nucl Med Mol Imaging 37: 954-961, 2010.
49. Li L, El-Hayek YH, Liu B, Chen Y, Gomez E, Wu X, Ning K, Li L, Chang N, Zhang L, *et al*: Direct-current electrical field guides neuronal stem/progenitor cell migration. Stem Cells 26: 2193-2200, 2008.
50. Luo Y: Cell-based therapy for stroke. J Neural Transm (Vienna) 118: 61-74, 2011.

51. Leu S, Lin YC, Yuen CM, Yen CH, Kao YH, Sun CK and Yip HK: Adipose-derived mesenchymal stem cells markedly attenuate brain infarct size and improve neurological function in rats. J Transl Med 8: 63, 2010.
52. Yoo J, Seo JJ, Eom JH and Hwang DY: Effects of stromal cell-derived factor 1α delivered at different phases of transient focal ischemia in rats. Neuroscience 209: 171-186, 2012.
53. Dziembowska M, Tham TN, Lau P, Vitry S, Lazarini F and Dubois-Dalcq M: A role for CXCR4 signaling in survival and migration of neural and oligodendrocyte precursors. Glia 50: 258-269, 2005.
54. Feng J, Liu J, Zhang X, Zhang L, Jiang J, Nolta J and Zhao M: Guided migration of neural stem cells derived from human embryonic stem cells by an electric field. Stem Cells 30: 349-355, 2012.
55. Chiazza F, Tammen H, Pintana H, Lietzau G, Collino M, Nyström T, Klein T, Darsalia V and Patrone C: The effect of DPP-4 inhibition to improve functional outcome after stroke is mediated by the SDF-1α/CXCR4 pathway. Cardiovasc Diabetol 17: 60, 2018.
56. Sun W, Liu J, Huan Y and Zhang C: Intracranial injection of recombinant stromal-derived factor-1 alpha (SDF-1α) attenuates traumatic brain injury in rats. Inflamm Res 63: 287-297, 2014.
57. Lu X, Bao X, Li J, Zhang G, Guan J, Gao Y, Wu P, Zhu Z, Huo X and Wang R: High-frequency repetitive transcranial magnetic stimulation for treating moderate traumatic brain injury in rats: A pilot study. Exp Ther Med 13: 2247-2254, 2017.
58. Salcedo L, Lian L, Jiang H, Sopko N, Penn M, Damaser M and Zutshi M: Low current electrical stimulation upregulates cytokine expression in the anal sphincter. Int J Colorectal Dis 27: 221-225, 2012.
59. George PM and Steinberg GK: Novel stroke therapeutics: Unraveling stroke pathophysiology and its impact on clinical treatments. Neuron 87: 297-309, 2015.
60. Belayev L, Hong S, Menghani H, Marcell SJ, Obenaus A, Freitas RS, Khoutorova L, Balaszczuk V, Jun B, Oriá RB and Bazan NG: Docosanoids promote neurogenesis and angiogenesis, blood-brain barrier integrity, penumbra protection, and neurobehavioral recovery after experimental ischemic stroke. Mol Neurobiol 55: 7090-7106, 2018.
61. Shohayeb B, Diab M, Ahmed M and Ng DCH: Factors that influence adult neurogenesis as potential therapy. Transl Neurodegener 7: 4, 2018.
62. Nih LR, Deroide N, Leré-Déan C, Lerouet D, Soustrat M, Levy BI, Silvestre JS, Merkulova-Rainon T, Pocard M, Margaill I and Kubis N: Neuroblast survival depends on mature vascular network formation after mouse stroke: Role of endothelial and smooth muscle progenitor cell co-administration. Eur J Neurosci 35: 1208-1217, 2012.
63. Yoon KJ, Lee Y and Han TR: Mechanism of functional recovery after repetitive transcranial magnetic stimulation (rTMS) in the subacute cerebral ischemic rat model: Neural plasticity or anti-apoptosis? Exp Brain Res 214: 549-556, 2011.
64. Guo F, Lou J, Han X, Deng Y and Huang X: Repetitive transcranial magnetic stimulation ameliorates cognitive impairment by enhancing neurogenesis and suppressing apoptosis in the hippocampus in rats with ischemic stroke. Front Physiol 8: 559, 2017.
65. Czeh B, Welt T, Fischer AK, Erhardt A, Schmitt W, Müller MB, Toschi N, Fuchs E and Keck ME: Chronic psychosocial stress and concomitant repetitive transcranial magnetic stimulation: effects on stress hormone levels and adult hippocampal neurogenesis. Biol Psychiatry 52: 1057-1065, 2002.